doi: 10.1038/nature07315

Structure of the guide-strand-containing Argonaute silencing complex

Yanli Wang[1], Gang Sheng[1], Stefan Juranek[2], Thomas Tuschl[2] and Dinshaw J. Patel[1]

[1]Structural Biology Program
Memorial Sloan-Kettering Cancer Center
New York, NY, 10065

[2]Howard Hughes Medical Institute
Laboratory of RNA Molecular Biology
The Rockefeller University
New York, NY, 10065

Supplementary Materials

Text

Divalent cation coordination to catalytic Asp residues

We did not observe a bound divalent cation coordinated to the catalytic Asp residues D546, D478 (on adjacent β-strands) and D660 of the PIWI domain of *T. thermophilus* Ago bound to the 21-mer DNA guide strand (Supplementary Fig. 11) as was observed previously for *A. aeolicus* Ago[14] and Mn-soaked crystals of *P. furiosus* Ago[13]. Since two divalent cations are normally asymmetrically coordinated to the catalytic Asp residues in RNase H mediated cleavage of DNA-RNA hybrids[24], a pair of cations would need to accompany insertion of the mRNA strand inside the *T. thermophilus* Ago catalytic pocket on ternary complex formation.

Conformational transitions

We observe hinge movements between the Mid and PIWI domains as part of significant conformational changes on proceeding from the 10-mer DNA guide strand complex with an anchored 3'-end (lighter colors in Fig. 3c) to the 21-mer DNA guide strand complex with both 5'- and 3'-anchored ends (darker colors in Fig. 3c). This contrasts with studies on *A. fulgidus* Piwi protein (contains Mid and PIWI domains, but lacks the N and PAZ domains and linker L1), where the protein structure remained unchanged on proceeding from the free[28] to the siRNA bound[20,21] state. This could in part reflect the difference in constraints on complex formation on proceeding from the single lobe scaffold of the smaller Piwi (lacks a PAZ-binding pocket), which contacts only one face of the bound duplex, to that of the bilobal scaffold of the larger Ago, which encircles the bound duplex.

A pair-wise comparison of the Mid-PIWI interface (superpositioned on the PIWI domain) in known structures of Piwi[28] and Ago[12,14] proteins in the free state, including guide DNA strand bound Ago complexes reported in this study, is outlined in Supplementary Fig. 12. Somewhat unexpectedly, the relative dispositions of the Mid and PIWI domains in the *A. fulgidus* Piwi protein is very similar to the *T. thermophilus* Ago binary complex with 21-mer DNA guide strand (Supplementary Fig. 12g). The C-terminus of the *T. thermophilus* Ago protein is disordered in the 10-mer DNA guide

strand complex, and hence the 5'-phosphate binding pocket in the Mid domain must be disrupted in the absence of an inserted C-terminal carboxylate group.

Supplementary Table 1. Data collection and refinement statistics

	Native Ago-10-mer DNA complex	Native Ago-21-mer DNA complex	SeMet-Ago-10-mer DNA complex	
Data Collection				
Space group	$P2_1$	$P2_12_12_1$	$P2_1$	
Cell dimensions				
a, b, c (Å)	77.82, 123.33, 84.89	74.74, 114.63, 175.69	77.90, 123.77, 84.84	
α, β, γ (°)	90.0, 95.7, 90.0	90.0, 90.0, 90.0	90.0, 95.2, 90.0	
			Peak	*Inflection*
Wavelength (Å)	0.97934	0.97926	0.97918	0.97929
Resolution (Å)	50-2.7 (2.8-2.7)*	50-3.0 (3.1-3.0)	50-3.3 (3.4-3.3)	50-3.7 (3.8-3.7)
R_{sym}	4.8 (58.0)	9.5 (45.5)	10.1 (54.1)	9.0 (27.0)
$I/\sigma I$	35.3 (2.5)	14.0 (2.0)	16.0 (3.6)	16.3 (5.3)
Completeness (%)	97.4 (100)	98.9 (97.3)	92.9 (100)	96.5 (89.7)
Redundancy	4.9 (5.0)	4.6 (4.4)	7.1 (7.3)	6.1 (2.7)
Refinement				
Resolution (Å)	30-2.7	30-3.0		
No. reflections	40,541	30,932		
R_{work}/R_{free}	23.6/29.7	22.6/28.6		
No. atoms				
Protein	9,139	10,307		
Ligand/ion	209	649		
Water	99	74		
B-factors				
Protein	53.3	57.0		
Ligand/ion	68.8	81.4		
Water	68.5	36.6		
R.m.s. deviations				
Bond lengths (Å)	0.0120	0.0086		
Bond angles (°)	1.5	1.6		

* Highest resolution shell is shown in parenthesis.

T. thermophilus Argonaute

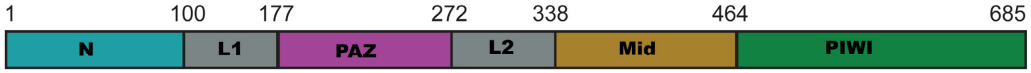

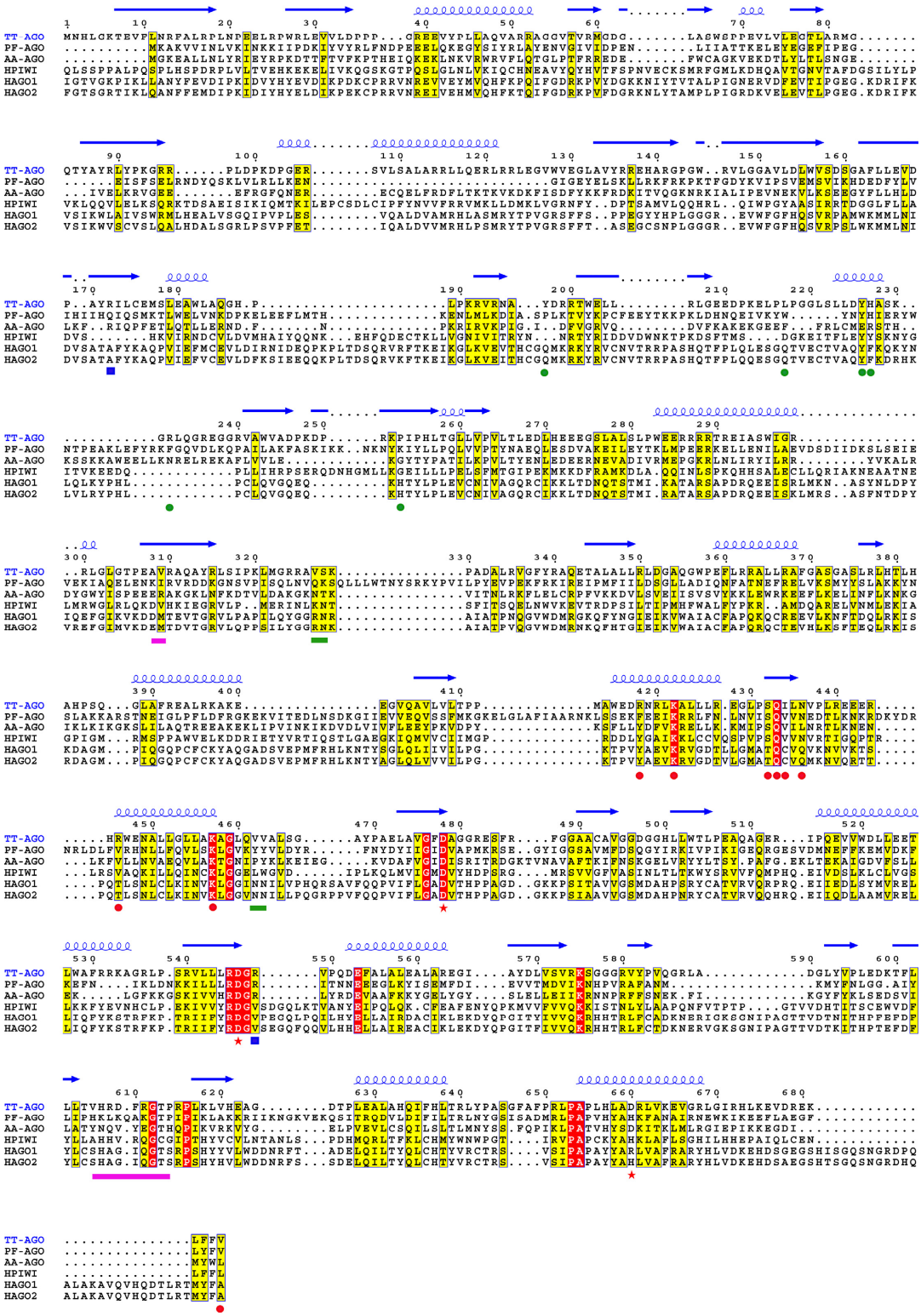

Supplementary Figure 1. Sequence alignment of Ago domains. The aligned sequences (Genebank ID, designated gi) are in the order of *Thermus thermophilus*-0026 (TtAgo, gi:46255097) *Pyrococcus furiosus*-0537 (PfAgo, gi:18976909), *Aquifex aeolicus*-1447 (AaAgo, gi:15606619), human PIWI (HsPIWI, gi:24431985), human Argonaute1 (HsAgo1, gi:6912352) and human Argonaute2 (HsAgo2, gi: 29171734). The secondary structure diagram for Tt-Ago is shown on the top, color coded by domains and linkers. Conserved residues are shaded in yellow, whereas essentially invariant residues are shown in red. Catalytic Asp residues are shown by red stars, binding residues in the Mid pocket are shown by red circles, binding residues in the PAZ pocket are shown by green circles and Arg residues contacting the 10-11 step are shown by blue squares. Residues involved in pivot motions on proceeding from the 10-mer DNA guide strand complex with an anchored 3'-end (lighter colors in Fig. 3c) to the 21-mer DNA guide strand complex with both 5'- and 3'-anchored ends (darker colors in Fig. 3c) are shown by pink (between PAZ and PIWI) and green (between Mid and PIWI) colored rectangles.

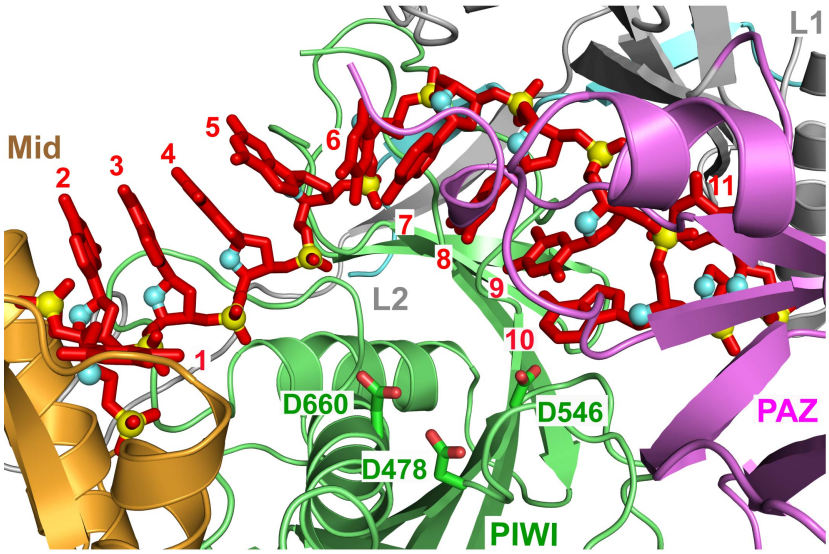

Supplementary Figure 2. . Stacking alignments in the *T. thermophilus* Ago bound to 21-mer DNA guide strand. Positioning of the RNase H catalytic D478, D546 and D660 residues of the PIWI domain relative to the stacked 2 to 10 segment of the bound guide strand.

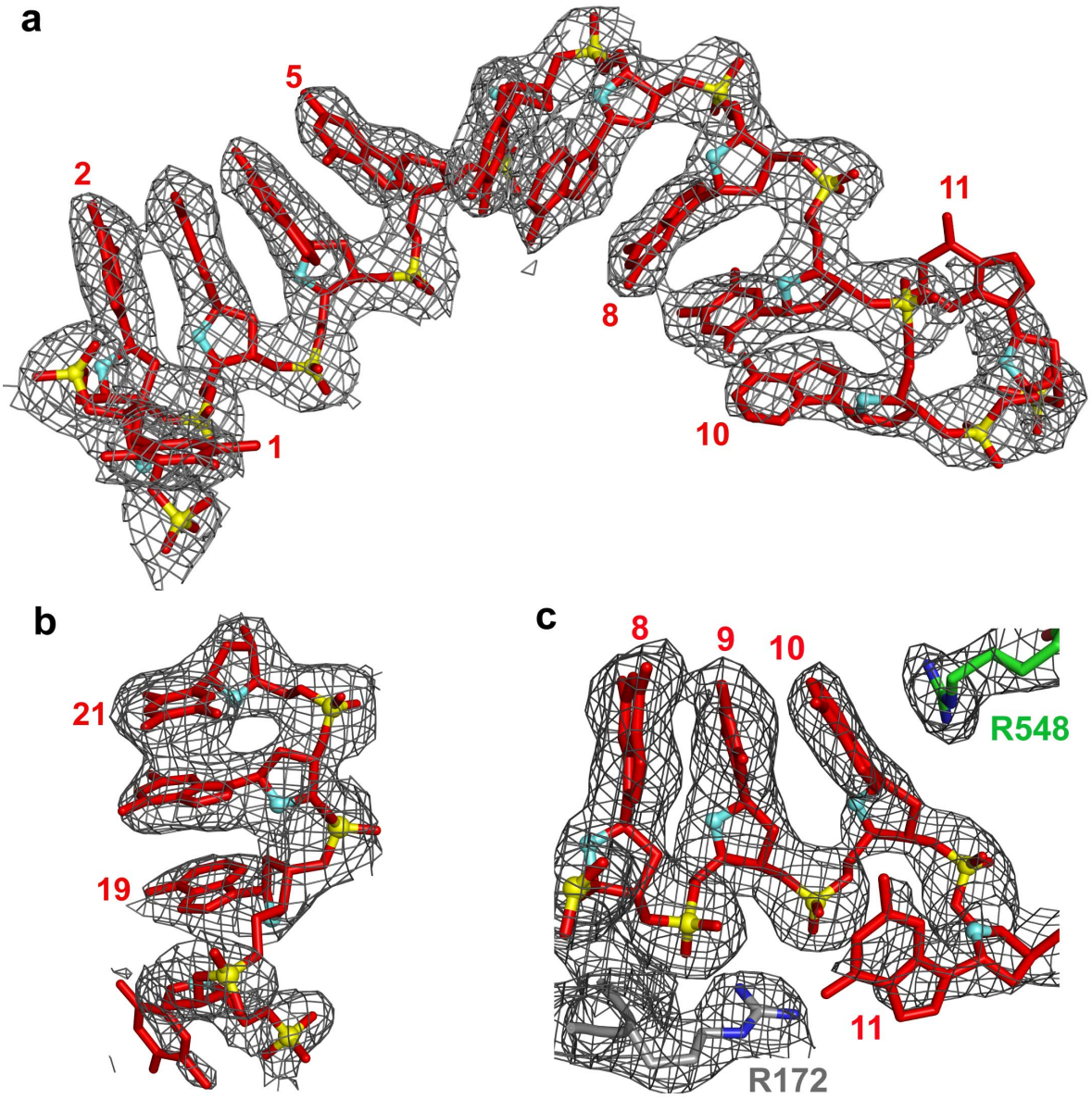

Supplementary Figure 3. Fitting the DNA into the electron density in the *T. thermophilus* Ago complex with bound 21-mer DNA guide strand. 2Fo-Fc electron density maps (1σ cut-off) of **a**, the 1-11 bound DNA segment, **b**, the 18-21 bound DNA segment and **c**, the bound DNA segment spanning residues 8-11, whereby the kink at the 10-11 step is promoted by interactions with Arg 172 and Arg 548.

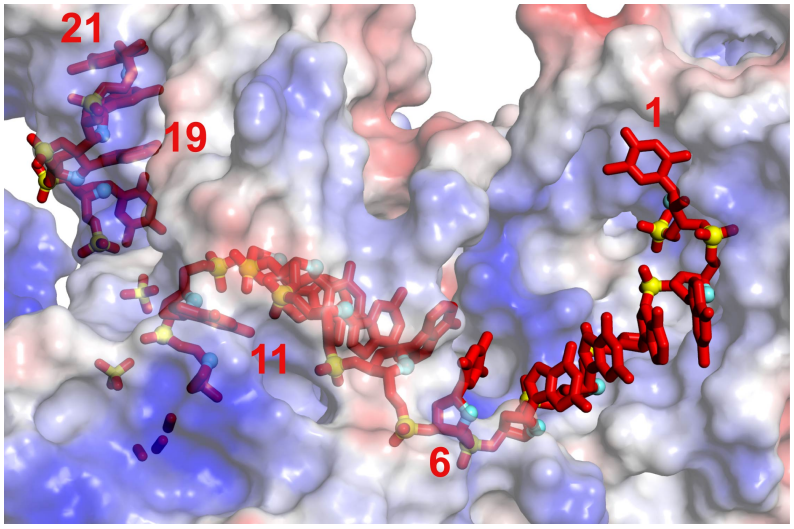

Supplementary Figure 4. Crystal structure of *T. thermophilus* Argonaute bound to 5'-phosphorylated 21-mer DNA guide strand. An expanded view of Fig. 1c with the protein in an electrostatic surface representation.

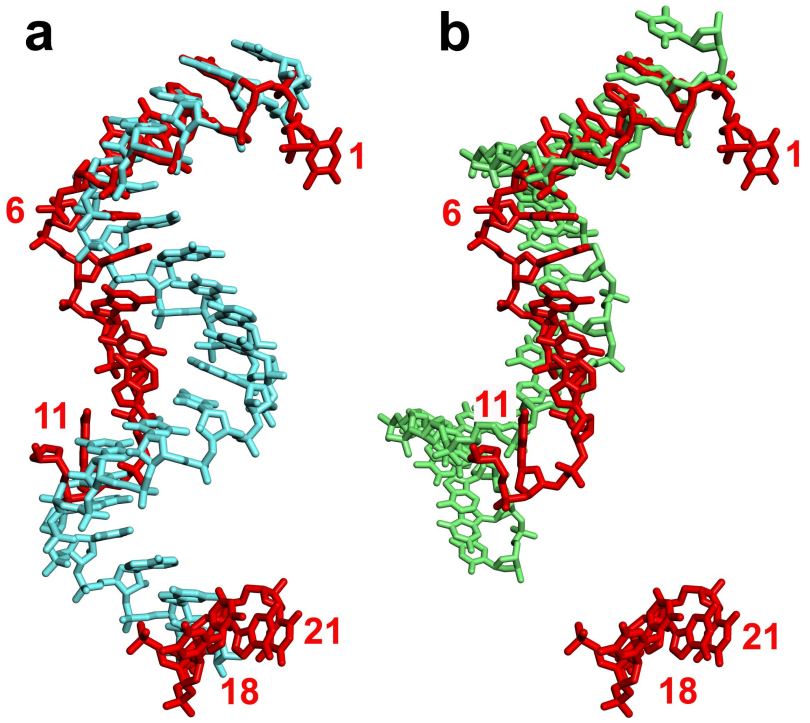

Supplementary Figure 5. Conformational changes in *T. thermophilus* Ago on formation of the 21-mer DNA guide strand complex. Superposition of segment 2 to 6 of the 21-mer DNA guide strand in the Ago complex (in red) with a 21-mer DNA strand adopting classical A-form RNA helix (in cyan) and B-form DNA helix (in green) conformations.

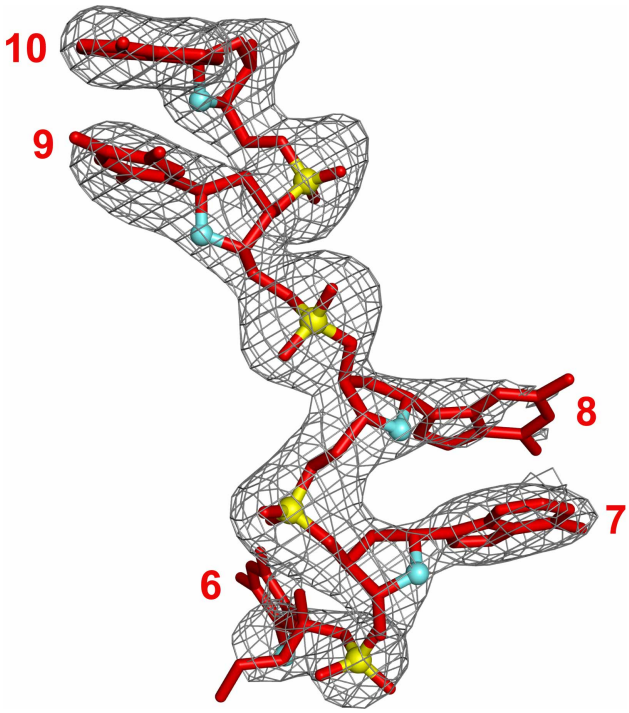

Supplementary Figure 6. Fitting the DNA into the electron density in the *T. thermophilus* Ago complex with bound 10-mer DNA guide strand. 2Fo-Fc electron density map (1σ cut-off) of the bound 6-10 DNA segment.

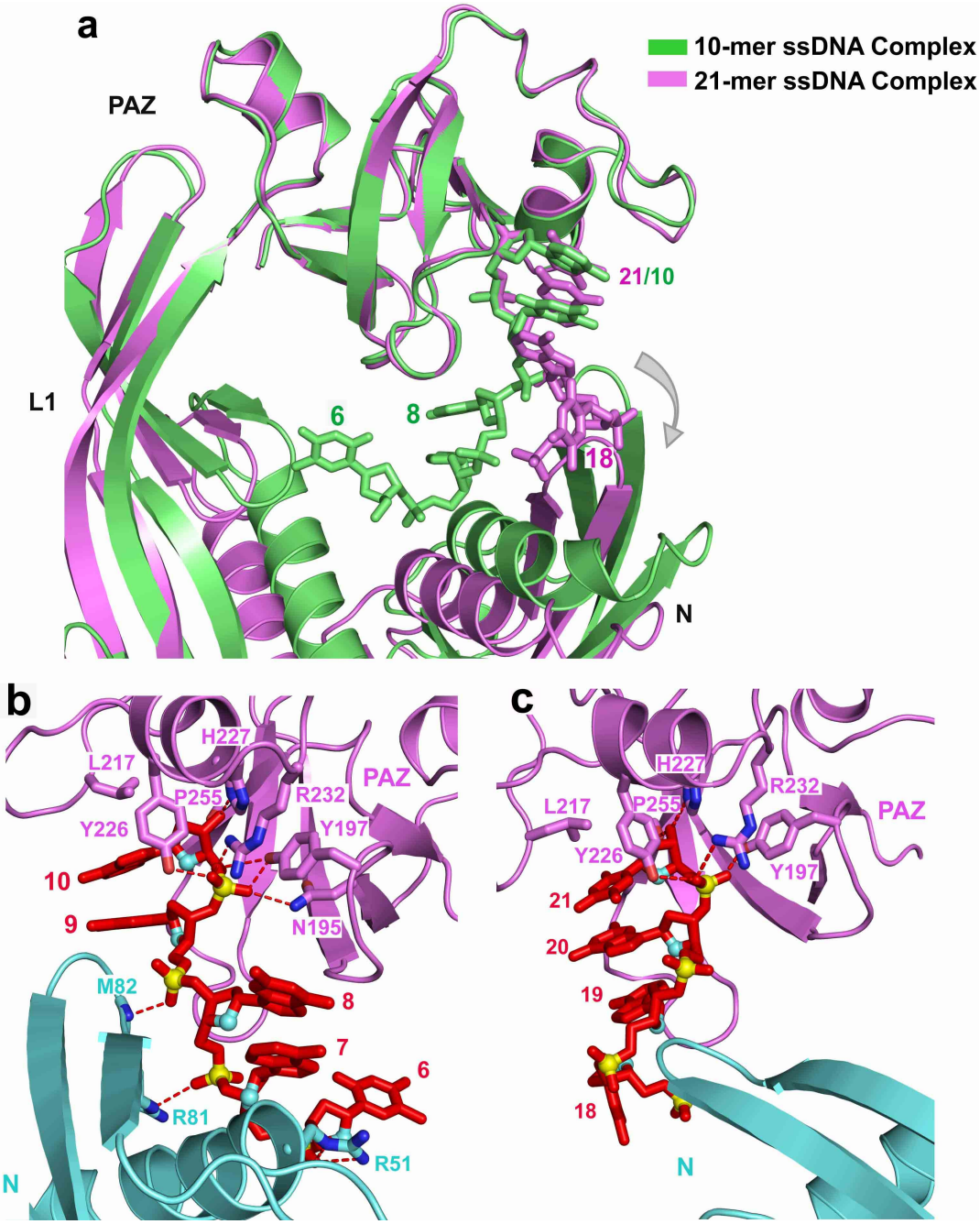

Supplementary Figure 7. DNA 3'-end trajectories in *T. thermophilus* Ago complexes with 10-mer and 21-mer DNA guide strands. **a**, A comparison of protein-DNA intermolecular contacts and N-PAZ interfaces in Ago complexes with 10-mer (colored green) and 21-mer (colored magenta) DNA guide strands, following superposition of their PAZ domains. **b,c** Intermolecular hydrogen-bonding alignments in Ago bound to the to 6 to 10 segment of the 10-mer DNA guide strand in (b) and to the 18 to 21 segment of the 21-mer DNA guide strand in (c).

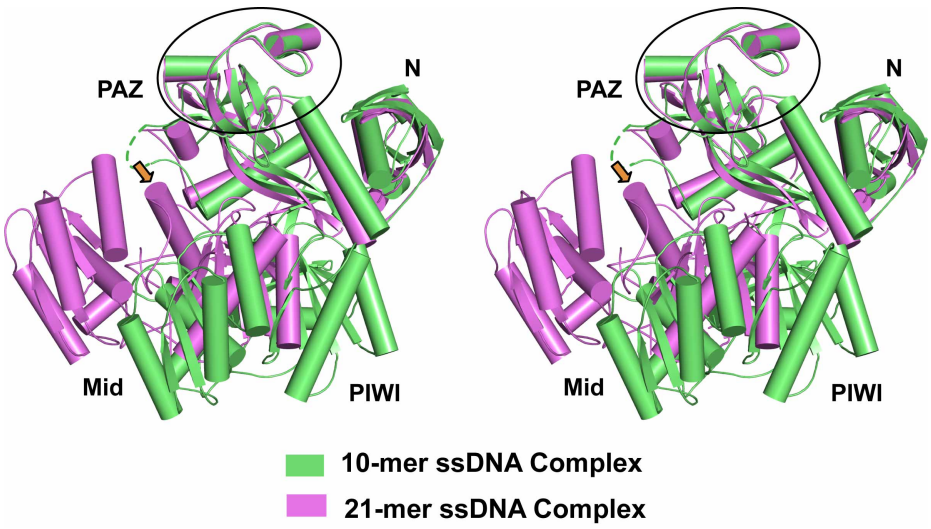

Supplementary Figure 8. Conformational changes in *T. thermophilus* Ago on formation of the 21-mer DNA guide strand complex. Stereo view of alignment of Agos in complexes with bound 10-mer (in green) and 21-mer (in magenta) DNA guide strands, following superpositioning of their PAZ domains (boxed segment). This stereo view emphasizes a different perspective from the mono view in Fig. 3c.The last α-helix and subsequent segment ending in the C-terminus of Ago is disordered in the 10-mer DNA guide strand complex, but is stable (designated by an arrow) in the 21-mer DNA guide strand complex.

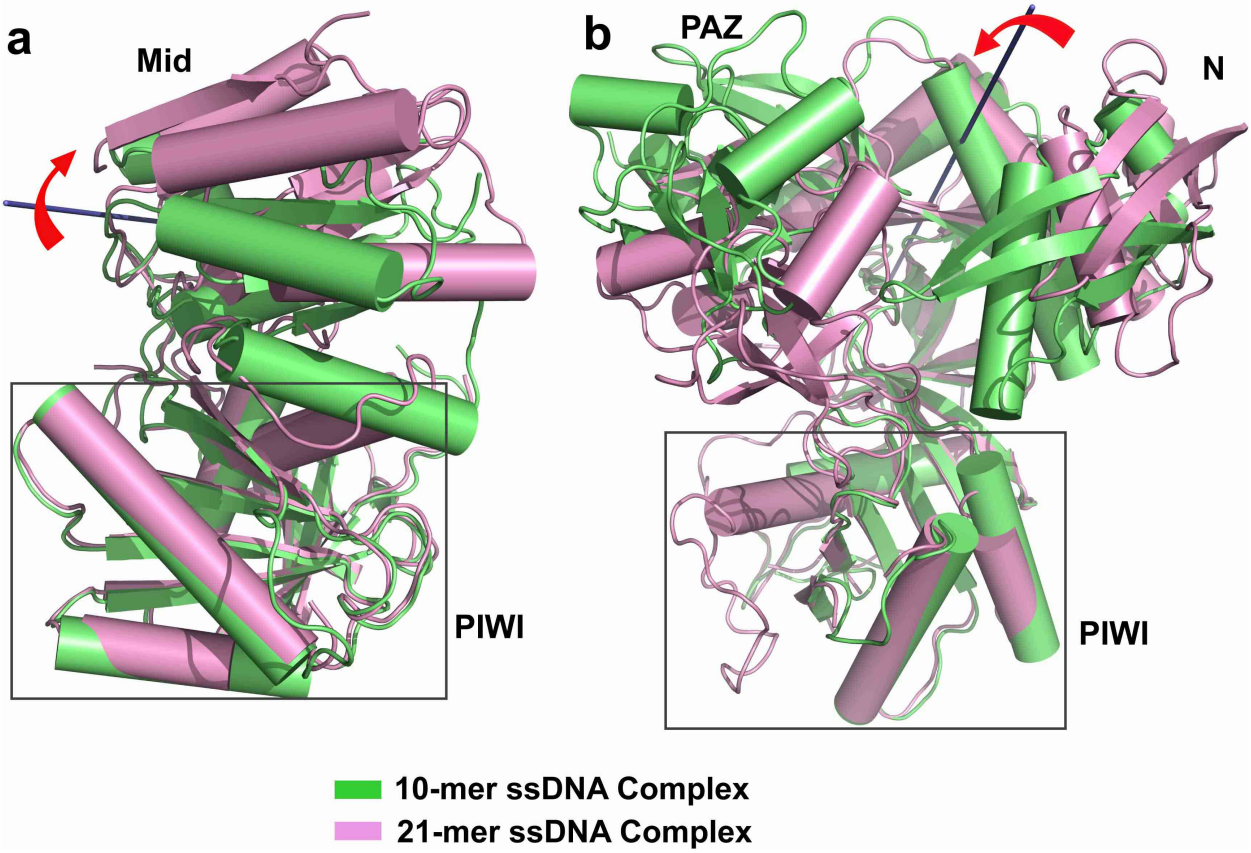

Supplementary Figure 9. Conformational transitions between *T. thermophilus* Ago in the 10-mer (colored green) and 21-mer DNA (colored magenta) guide strand complexes. **a**, Conformational transition (a 22^{o} rotation and 0.0 Å translation) in the Mid domain on superpositioning the PIWI domains. **b**, Conformational transition (a 25^{o} rotation and 0.4 Å translation) in the PAZ-containing lobe (PAZ and N domains and L1 linker) on superpositioning the PIWI domains.

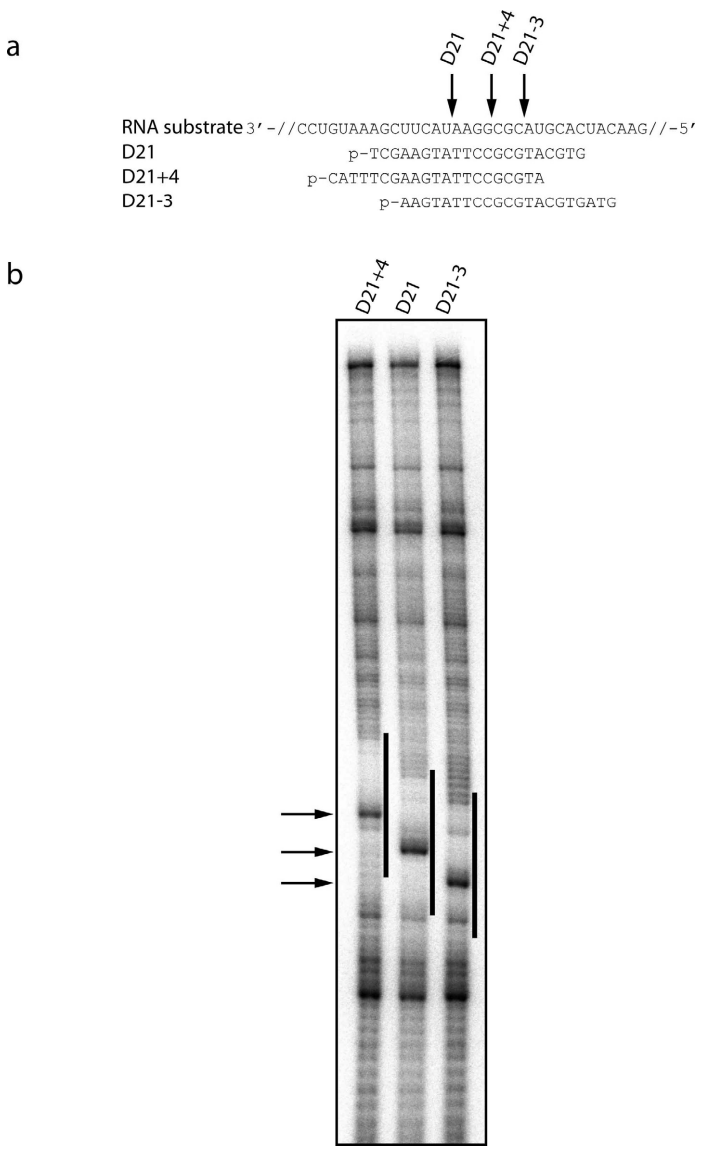

Supplementary Figure 10. Guide-strand-dependent cleavage of the RNA substrate by *T. thermophilus* Ago. **a**, The sequences of three different guide DNAs and the RNA cleavage substrate are shown ('p' indicates a 5'-phosphate). **b**, DNA guide strands were incubated with *T. thermophilus* Ago followed by addition of the 5'-radiolabeled RNA cleavage substrate. Reaction products were resolved using a 8% denaturing PAGE gel and monitored by phosphoimaging. Guide D21+4 was unable to guide target RNA cleavage. The region of cleavage substrate bound by the guide DNA is marked by the black bar left to each lane, while the cleavage position is indicated by arrows. As expected, the target RNA was cleaved in the center of the region covered by the guide DNA[27].

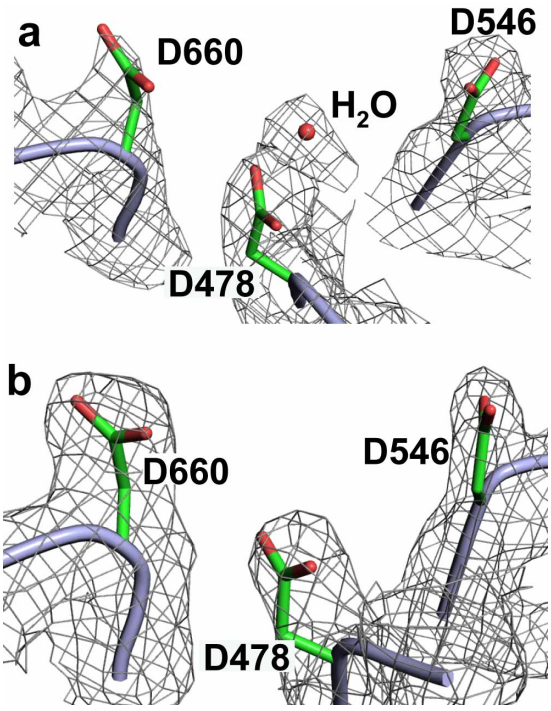

Supplementary Figure 11. Fitting the catalystic Asp residues into the electron density in the *T. thermophilus* Ago complex with bound 21-mer DNA guide strand. **a,b** 2Fo-Fc electron density maps (1σ cut-off) of Asp 478, Asp 546 and Asp 660 in the two molecules of the complex in the asymmetric unit.

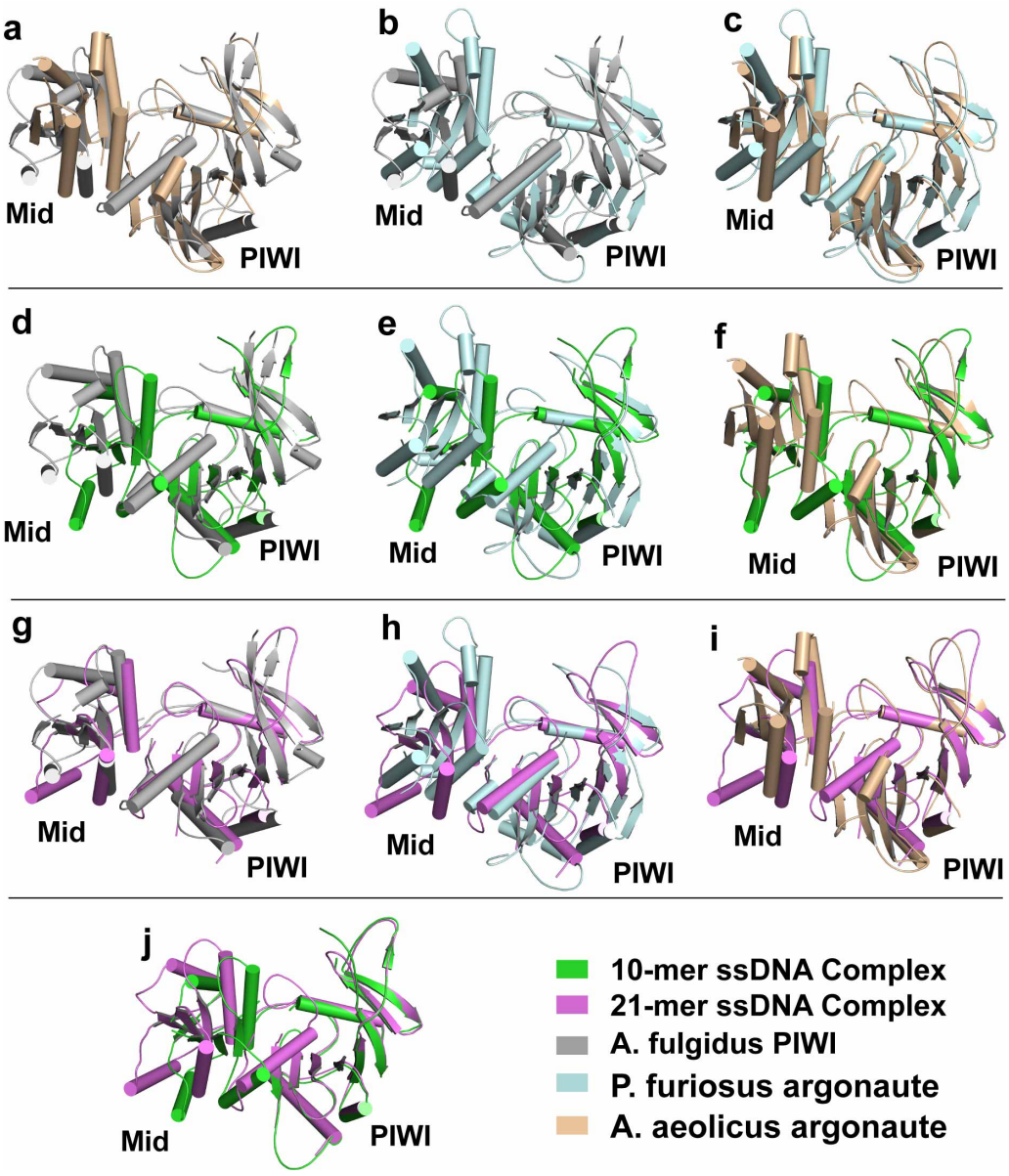

Supplementary Figure 12. Pair-wise comparisons of the Mid-PIWI interface in structures of Piwi and Ago complexes. The systems are color-coded as follows: *T. thermophilus* Ago bound to 10-mer DNA guide strand (green), *T. thermophilus* Ago bound to 21-mer DNA guide strand (magenta), *A. fulgidus* Piwi in the free state[28] (grey; id:1w9h), *P. furiosus* Ago in the free state[12] (cyan; id:1u04) and *A. aeolicus* Ago in the free state[14] (beige; id:1yvu). The pair-wise comparison is undertaken following superposition of the PIWI domain.